Biochimica et Biophysica Acta 1817 (2012) 2038–2048

Contents lists available at SciVerse ScienceDirect

Biochimica et Biophysica Acta

journal homepage: www.elsevier.com/locate/bbabio

Reactive oxygen species affect ATP hydrolysis by targeting a highly conserved amino acid cluster in the thylakoid ATP synthase γ subunit

Felix Buchert [a], Yvonne Schober [b], Andreas Römpp [b], Mark L. Richter [c], Christoph Forreiter [a,*]

[a] Department of Plant Physiology, Justus-Liebig-University Giessen, Senckenbergstr. 3, 35390 Giessen, Germany
[b] Institute of Inorganic and Analytical Chemistry, Justus-Liebig-University Giessen, Schubertstr. 60, 35392 Giessen, Germany
[c] Department of Molecular Biosciences, The University of Kansas, 1200 Sunnyside Ave., Lawrence, KS 66045, USA

ARTICLE INFO

Article history:
Received 6 March 2012
Received in revised form 8 June 2012
Accepted 12 June 2012
Available online 19 June 2012

Keywords:
(Chloroplast) F-type ATP synthase
Singlet oxygen
Hydrogen peroxide
Reactive oxygen species

ABSTRACT

The vast majority of organisms produce ATP by a membrane-bound rotating protein complex, termed F-ATP synthase. In chloroplasts, the corresponding enzyme generates ATP by using a transmembrane proton gradient generated during photosynthesis, a process releasing high amounts of molecular oxygen as a natural byproduct. Due to its chemical properties, oxygen can be reduced incompletely which generates several highly reactive oxygen species (ROS) that are able to oxidize a broad range of biomolecules. In extension to previous studies it could be shown that ROS dramatically decreased ATP synthesis *in situ* and affected the CF1 portion *in vitro*. A conserved cluster of three methionines and a cysteine on the chloroplast γ subunit could be identified by mass spectrometry to be oxidized by ROS. Analysis of amino acid substitutions in a hybrid F1 assembly system indicated that these residues were exclusive catalytic targets for hydrogen peroxide and singlet oxygen, although it could be deduced that additional unknown amino acid targets might be involved in the latter reaction. The cluster was tightly integrated in catalytic turnover since mutants varied in MgATPase rates, stimulation by sulfite and chloroplast-specific γ subunit redox-modulation. Some partial disruptions of the cluster by mutagenesis were dominant over others regarding their effects on catalysis and response to ROS.

1. Introduction

In plants, especially under high light conditions, the electron transfer chain is frequently overloaded. As a consequence, triplet excited pigments are generated which can produce different reactive oxygen species (ROS) and other radicals [reviewed in 1]. These highly reactive molecules can damage the photosynthetic apparatus and promote photoinhibition [2]. Usually ROS are scavenged by various antioxidative defense mechanisms [3,4], but the equilibrium between production and scavenging is permanently perturbed upon environmental changes. The most prominent ROS formed under high light conditions is hydrogen peroxide (H_2O_2), mainly formed by superoxide dismutase at photosystem I, and singlet oxygen ($^1O_2$), mainly produced by triplet chlorophyll during energy transfer at photosystem II. There are indications that transport of H_2O_2 is facilitated via aquaporins [5], enabling the molecule to diffuse rapidly within the photosynthetic cell. The transport mechanism for $^1O_2$ is still unclear, but recent studies suggest that $^1O_2$ can also reach different cellular compartments distant from its origin [6]. Thus, tight control of ROS is of upmost importance to maintain a functionally active photosynthetic machinery under high light stress. Therefore, it is not surprising that ROS are also considered to act as signaling molecules [7,8] allowing an adjusted cellular response to increasing ROS levels.

The chloroplast ATP synthase [reviewed in 9] is closely related to its bacterial and mitochondrial homologs. Due to high overall structural similarity and amino acid homology in functionally important domains, it is assumed that F-ATP synthases share a common ancestor. Like all F-type ATP synthase members, the chloroplast enzyme is composed of two functional portions. In a reversible process ATP is synthesized or hydrolyzed by the peripheral membrane protein complex CF1, utilizing or generating a proton gradient by H^+ translocation through an integral membrane-spanning CFO protein complex. Spinach (*Spinacia oleracea*) CFO portion consists of four different subunits with a stoichiometry of $I_1II_1III_{14}IV_1$. The copy number of subunit III is species-specific. CF1 is an assembly of five subunits, having a stoichiometry of $\alpha_3\beta_3\gamma_1\delta_1\varepsilon_1$. Enzyme activity is tightly coupled to rotation of γ, ε and the subunit III-ring, while ATP synthesis and hydrolysis are restricted to three of the six nucleotide binding sites located at each α/β interface. A special feature of higher plant CF1 is an additional regulatory domain in the γ subunit consisting of about 40 amino acids. The regulatory core element is a disulfide forming pair of cysteines, designated as C199 and C205 in spinach. Reduction of the γ disulfide elevates ATP hydrolysis and synthesis, probably via an inter-domain movement within the γ subunit

Abbreviations: CF1, MF1, EcF1, RrF1, TF1, coupling factor 1 enzymes from chloroplasts, mitochondria, *Escherichia coli*, *Rhodospirillum rubrum* and thermophilic *Bacillus* PS3; FO, coupling factor O; CFO, chloroplast coupling factor O; hybrid F1, recombinant photosynthetic F1 core complex consisting of RrF1 $\alpha_3\beta_3$ hexamer and *Spinacia oleracea* CF1 γ subunit; Pi, inorganic phosphate; ROS, reactive oxygen species; $^1O_2$, singlet oxygen; H_2O_2, hydrogen peroxide; DTT, Dithiothreitol; $CuCl_2$, Copper (II) chloride

* Corresponding author. Tel.: +49 641 9935436; fax: +49 641 9935429.
E-mail address: christoph.forreiter@bot3.bio.uni-giessen.de (C. Forreiter).

0005-2728/$ – see front matter © 2012 Elsevier B.V. All rights reserved.
doi:10.1016/j.bbabio.2012.06.007

that concurrently might coordinate an additional regulatory interplay between γ and ε subunits. It is assumed that catalytic activity of CF1 is tightly redox-regulated to prevent futile ATP hydrolysis in the dark when ATP synthesis is inactive.

Previously, it was shown that F-ATP synthases from various organisms are susceptible to different reactive oxygen species *per se* [10–12]. This machinery is indispensable for oxidative phosphorylation and photophosphorylation in a ROS producing cellular environment of aerobic organisms [1,13,14]. It was shown that ATP synthase disorders promote ROS generation in mitochondria [15]. In plants, kinetic alterations of the ATP synthase can modulate non-photochemical quenching [16] which is a mechanism to minimize ROS-promoted photoinhibition [2]. However, a direct effect of ROS on non-photochemical quenching by affecting ATP synthase remains elusive. In this study, previous findings [12,17] were extended by identification of specific ROS targets within the CF1 γ subunit. The common target residues were located in a highly conserved methionine–cysteine cluster that is in part involved in coupling transmission of ATP hydrolysis and proton translocation [18] and forms a contact with both the empty and the ADP-containing β subunits [19–21]. Integrity of the cluster was essential since even minimally perturbing substitutions of the target amino acids caused aberration of nucleotide release during catalytic turnover and plant specific redox-modulation by γ disulfide reduction. Concomitantly, the cluster mutants rendered the enzyme significantly less sensitive to ROS. Catalytic properties as well as ROS responses of certain mutations were dominant over others, indicating that cluster residues were interdependent. Additionally, different ROS varied in their impact, since ROS responses of disrupted cluster mutants were inverted depending on the oxidant. In general, the results supported the hypothesis that F-ATP synthases contain a versatile ROS target cluster of highly conserved and critically placed amino acids.

2. Materials and methods

2.1. Reagents

Ampicillin, Chloramphenicol, DTT, 2-Amino-2-hydroxymethyl-propane-1,3-diol (Tris), 2-(N-morpholino)-ethanesulfonic acid (MES), N-(2-Hydroxy-1,1-bis(hydroxymethyl) ethyl) glycine (Tricine), magnesium chloride ($MgCl_2$), Rose Bengal (RB) and Plas/mini Isolation Spin-Kit were purchased from AppliChem (Darmstadt, Germany). $CuCl_2$, dihydrate was purchased from Merck (Hohenbrunn, Germany). Adenosine-5′-triphosphate (ATP), adenosine 5′-(trihydrogen diphosphate) (ADP), glycerol and ultra pure urea were purchased from Roth (Karlsruhe, Germany). Superflow Ni-NTA agarose was obtained from QIAGEN (Hilden, Germany). HPLC grade water, puriss grade, formic acid (FA) and purum grade hydrogen peroxide solution (H_2O_2) were obtained from Fluka (Neu-Ulm, Germany). Uvasol® acetonitrile (MeCN), ReagentPlus™ ammonium bicarbonate (NH_4HCO_3), potassium phosphate (K_2HPO_4/KH_2PO_4), sodium chloride (NaCl) and sodium sulfite (Na_2SO_3) were purchased from Sigma (Steinheim, Germany). Trypsin (Sequencing Grade Modified Trypsin, porcine) was purchased from Promega (Madison, WI, USA). Oligonucleotides were synthesized by Invitrogen (Darmstadt, Germany). T4 Polynucleotide Kinase, *Dpn*I and T4 DNA ligase were purchased from New England Biolabs (Frankfurt/Main, Germany). Phusion DNA polymerase was obtained from Fisher Scientific (Schwerte, Germany).

2.2. Alignment of F1 γ subunits

Multiple sequence alignment and phylogenetic tree calculations were done using ClustalW [22] and Geneious [23], respectively. Visualization of a structural alignment was performed using PyMOL/CEalign [24,25]. The homology model of spinach CF1 γ subunit [26] and the crystal structure of spinach CF1 α and β subunits [27; PDB ID: 1FX0] were aligned to a template structure [28; PDB ID: 3OAA] of corresponding *E. coli* F1 subunits.

2.3. Plant material, isolation of CF1 and subunit dissection

Thylakoid membrane isolation from fresh spinach (*S. oleracea*) leaves was carried out as described earlier [12,29]. Isolation of catalytically active spinach CF1 [30], followed by the release of δ and ε subunit [31], was performed according to published procedures. Determination of protein, using bovine serum albumin as a standard, and chlorophyll concentrations were carried out according to the methods of Bradford [32] and Arnon [33], respectively.

2.4. Mass spectrometry analysis

ROS treated soluble spinach CF1 (see Section 2.8) was frozen in liquid nitrogen and kept on ice. CF1 was digested using modified trypsin at a 1:30 enzyme/protein (w/w) ratio at 37 °C for 15 h. In addition, a purification step using C18 Zip Tips (Varian, Lake Forest, USA) was applied according to the manufacturer's recommendations. Measurements of all samples were accomplished on an Ultimate binary nano HPLC pump/autosampler system for HPLC analysis (LCPackings/Dionex, Idstein, Germany). 5 μL of the sample were pre-focused on a trap column (Dionex, C18 PepMap, inner diameter 300 μm, length 5 mm) and separated on a fused-silica C18 PepMap100 capillary column (Dionex, 3 μm, 100 Å; inner diameter 75 μm; length 150 mm). The flow rate was 0.2 μL min^{-1}. The nanoHPLC system was coupled either to a nanoelectrospray interface of a LTQ Orbitrap Discovery mass spectrometer or a LTQ FT Ultra mass spectrometer (both Thermo Fisher Scientific GmbH, Bremen, Germany). Survey MS scans with a high mass accuracy better than 2 ppm were measured on both instruments. The three most intense peaks in the survey scan were chosen for fragmentation in ion trap ms mode. Collision induced fragmentation was used for fragmentation in the ion trap. Each sample was measured three times. LC–ESI–MS/MS data were searched against the UniProt database (www.uniprot.org) of spinach CF1 using Proteome Discoverer 1.2 (Thermo Fisher Scientific GmbH, Bremen, Germany) based on the SEQUEST search algorithm. Mass tolerance for precursor ions was set to 2 ppm, mass tolerance for fragment ions was set to 0.8 u. Two missed cleavages were allowed in order to account for incomplete digestion. Oxidation was allowed as post translational modification. Peptides with a "peptide probability" (SEQUEST parameter) of 50 and higher were considered as significant identifications. Peptides of interest where manually inspected, based on fragment ion spectra and the specific location of oxidized amino acid residues was verified.

2.5. Site-directed mutagenesis

All mutations were performed using template plasmids carrying a cDNA coding for spinach CF1 γ subunit [34] and wild type *Rhodospirillum rubrum* β subunit [35]. Phosphorylation of 5′-end abutting oligonucleotides, PCR reaction, restriction digest of the template DNA, ligation of the amplified pET vector and transformation into *E. coli* XL1-Blue cells, followed by selection for ampicillin resistance (100 μg mL^{-1}), were carried out according to the manufacturer's instructions. Sequencing was performed by GATC Biotech (Konstanz, Germany). Oligonucleotide sequences are shown in Supplementary Table S1. Additionally, a previously published plasmid [36] was used, coding for an alanine substitution of disulfide-forming regulatory cysteines (γC199 + 205A).

2.6. Protein expression and purification

The pET plasmids carrying recombinant spinach CF1 γ subunit and previously published plasmids carrying *R. rubrum* F1 α subunit with an N-terminal His-tag [37] and wild type *R. rubrum* β subunit [35] were transformed into expression host *E. coli* BL21(DE3)/pLysS [38].

Cells were selected for ampicillin (100 μg mL^{-1}) and chloramphenicol (34 μg mL^{-1}) resistance. Cell suspensions were passed three times through a French press at 10,000 psi for lysis. Inclusion bodies were purified as described elsewhere [34] and stored at −80 °C in 25 mM Tris–HCl (pH 8.0), 1 mM EDTA and 50% (v/v) glycerol until further usage.

2.7. Hybrid F1 assembly

Assembly of a catalytically active hybrid F1 $\alpha^{R}{}_{3}\beta^{R}{}_{3}\gamma^{C}$ core complex consisting of RrF1 α_{6xHis} (α^{R}) and β (β^{R}) subunits and spinach CF1 γ (γ^{C}) subunit was performed based on a method described elsewhere [39]. Briefly, inclusion bodies of the subunits were solubilized in 8 M urea, centrifuged at 16,000 rpm and 4 °C for 30 min and mixed at a ratio of $\alpha^{R}:\beta^{R}:\gamma^{C}=5:5:3$ by weight. The subunit mix was diluted to 0.1 mg protein mL^{-1} in refolding buffer containing 4 M urea, 50 mM Tris–HCl (pH 8.0), 50 mM NaCl, 50 mM $MgCl_2$, 50 mM ATP, 20 mM DTT and 20% glycerol and dialyzed in two steps at 4 °C against 10 volumes dialysis buffer containing 50 mM Tris–HCl (pH 8.0), 50 mM NaCl and 20% (v/v) glycerol. The dialyzed protein was applied to a Ni-NTA affinity column equilibrated with 50 mM Tris–HCl (pH 8.0), 50 mM NaCl and 1 mM ATP (TNA buffer), washed and eluted in TNA buffer including 300 mM imidazole. Eluted protein was precipitated by adding solid ammonium sulfate (50% saturation) and desalted after centrifugation via Sephadex G50 spin columns [40]. Assemblies were stored in aliquots at −80 °C in TAG buffer containing 50 mM Tris–HCl (pH 8.0), 1 mM ATP and 20% (v/v) glycerol.

2.8. Treatment with reactive oxygen species

Singlet oxygen ($^1O_2$) exposure of thylakoid membranes was carried out as described previously [12]. Soluble chloroplast and hybrid F1 were illuminated for various periods in the presence of 2 μM RB. Hydrogen peroxide (H_2O_2) exposure was carried out for 60 min at 37 °C and various concentrations of H_2O_2. Hydrogen peroxide can be activated by several compounds including transition-metal ions yielding hydroxyl radicals via Fenton chemistry [41]. Therefore any catalysts were omitted in the assay resulting in rather high concentrations of H_2O_2 applied. The reaction was quenched for 30 min at 25 °C by 12.5-fold dilution containing 50 mM Tris–HCl (pH 8.0) and 10 mM L-methionine. The concentration of the enzyme during ROS treatment was 0.29 μM in TA buffer containing 50 mM Tris–HCl (pH 8.0) and 1 mM ATP. Hybrid F1 was kept in TAG buffer during ROS exposure. In some experiments $^1O_2$ was generated in 50 mM MES-KOH (pH 6.0), 1 mM ATP and 20% (v/v) glycerol.

2.9. ATP hydrolysis and synthesis measurements

Activity measurements of spinach thylakoids and soluble chloroplast/hybrid F1 were based on the colorimetric determination of Pi [42]. Pretreatment of thylakoid membranes with DTT [29] was followed by exposure to $^1O_2$ [12]. The ATPase activity of thylakoids equivalent to 10 μg chlorophyll was assayed for 3 min at 37 °C in 0.5 mL reaction mixture containing 50 mM Tricine–NaOH (pH 8.0), 40 mM Na_2SO_3, 10 mM NaCl, 3 mM ATP and 1.5 mM $MgCl_2$. Photophosphorylation after $^1O_2$ exposure was assayed [43] using an RG2 transmission filter (Schott, Mainz, Germany) to avoid continuous excitation of RB. MgATP hydrolysis by CF1, CF1-δε and hybrid F1 assemblies was carried out in a 0.5 mL reaction volume containing 2–5 μg of protein in 50 mM Tris–HCl (pH 8.0), 25 mM Na_2SO_3, 5 mM ATP and 2.5 mM $MgCl_2$. Sodium sulfite was omitted in some experiments. Addition of 0.5 mL trichloroacetic acid terminated the reaction. Samples were assayed for Pi release immediately and after incubation at 37 °C for 2 min. Hybrid F1 was kept in TAG buffer. In some experiments 0.29 μM hybrid F1 was incubated in TAG buffer for 60 min and 37 °C in the presence of 10 mM DTT (reduction) or 100 μM $CuCl_2$ (oxidation), respectively. Desalted [40] ammonium sulfate precipitates of CF1 and CF1-δε were reduced for 90 min and 25 °C in TA buffer and 10 mM DTT at an enzyme concentration of 1.16 μM.

3. Results

3.1. Impact of singlet oxygen on enzyme activity in situ and in vitro

Supporting and extending a previous analysis [12], an initial experiment revealed that both, ATP hydrolysis and ATP synthesis by spinach thylakoid membranes were affected by $^1O_2$ (Fig. 1A). The quantitative impact on both activities was comparable, resulting in residual ATP hydrolysis of 72% and ATP synthesis of 70% after treatment with 10 μM RB.

In order to prove that the suggested activity attenuation *in situ* [12] was primarily the result of oxidative damage of CF1, the catalytic portion was isolated from thylakoid membranes and tested for residual activity after $^1O_2$ treatment. The data indicated that activity of CF1 *in vitro* attenuated upon $^1O_2$ exposure (Fig. 1B). Although initial hints [17] suggest that the γ subunit is the primary target of $^1O_2$, it still remained unclear if the ε subunit was involved in the observed loss of activity *in situ* and *in vitro*. In order to rule out any involvement of ε in $^1O_2$-induced activity attenuation of CF1, the δ and ε subunits were removed to obtain CF1-δε. Due to the missing ε subunit [44], CF1-δε showed higher MgATPase activity than CF1 (Fig. 1B). CF1-δε was even more susceptible to $^1O_2$ than CF1.

3.2. Pinpointing putative targets of singlet oxygen using the homology model structure of CF1 γ subunit

A high resolution structure of the chloroplast F1 γ subunit is not available. Therefore, a homology model based on mitochondrial and bacterial F1 γ subunit structures has been developed [26]. This model served as a platform for spatial mapping of putative $^1O_2$ targets based on reported ROS-protein interactions with tyrosine, histidine and tryptophan, as well as cysteine and methionine [45]. An amino acid sequence alignment of sixteen F1 γ subunits (Fig. 2A) resulted in a sequence identity of only 7.4%. Such low identity is in good agreement with other alignments [46] and indicated that most of the conserved residues are restricted to the amino and carboxyl termini and a small central region. These regions were part of the structurally conserved terminal alpha-helical elements and a γ protrusion loop that contained a set of highly conserved methionines and a cysteine in close proximity. The ROS target mapping approach revealed that these sulfur-containing amino acids formed a cluster located at the "neck" region of the γ subunit that protruded from the $\alpha_3\beta_3$ hexamer (Fig. 2B, C). This cluster is highly conserved in other γ subunits and can be found in several published structures, for example those of bacterial [28; PDB ID: 3OAA], yeast mitochondrial [47; PDB ID: 2XOK] and bovine mitochondrial [48; PDB ID: 2WSS] F1 γ subunits. Depending on the organism, the cluster consists of one or two N-terminally located methionines, a central cysteine and one or two C-terminally located methionines. The methionines and the cysteine are located near the second "catch" region of the empty and ADP-containing β subunits that forms a contact with the γ subunit [19–21].

3.3. Mass spectrometry analysis of CF1 oxidation

Using LC–ESI–MS/MS, CF1 was analyzed for oxidized amino acid residues after ROS exposure. The data clearly indicated that the proposed candidates of the conserved amino acid cluster (Fig. 2) were specifically oxidized upon $^1O_2$ exposure (Fig. 3) since control samples did not contain modified cluster residues (Supplementary Fig. S1). Due to their sulfur atoms, methionine and cysteine are easily oxidized so these two residues are major sites of protein oxidation [49]. Methionine is successively oxidized at the sulfur center, forming methionine sulfoxide (mono-oxidation) and methionine sulfone (di-oxidation).

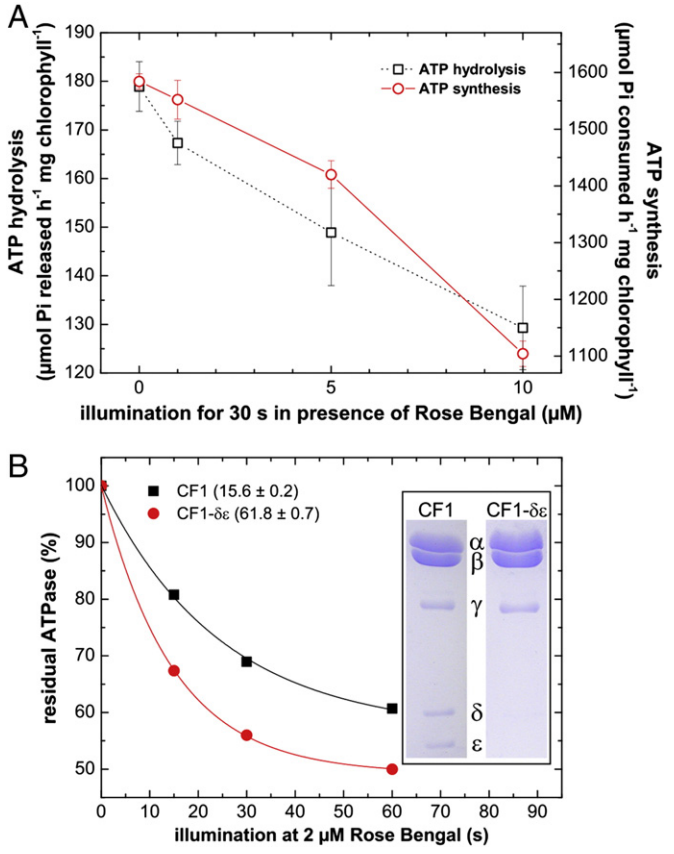

Fig. 1. Singlet oxygen lowered enzyme activity *in situ* and *in vitro*. Activities of three measurements (± standard error) are shown. (A) CF1CFO of isolated spinach thylakoid membranes was assayed for ATP synthesis (photophosphorylation) and sulfite-stimulated MgATP hydrolysis. (B) Sulfite-stimulated MgATP hydrolysis of isolated CF1 and CF1 lacking the δ and ε subunit (CF1-δε) is shown. MgATPase (expressed as μmol Pi released min^{-1} mg $protein^{-1}$) equal to 100% activity is given in brackets. The inset shows an SDS polyacrylamide gel with 6 μg of purified protein stained with Coomassie Brilliant Blue R-250.

Reactions with cysteines within proteins are more diverse and, for instance, result in the formation of a disulfide or oxyacid derivatives, such as tri-oxidized sulfonic acid. After treating the samples with $^1O_2$, N-terminal γM23 was oxidized to sulfoxide (Fig. 3A), whereas the C-terminal methionines were mutually affected: Peptide fragments containing a pair of γM279 and γM282 sulfoxides were detected (Fig. 3B). Additionally, fragments containing a mixture of methionine sulfoxide and methionine sulfone (Fig. 3C) were identified. Methionine sulfone of either γM279 or γM282 was only observed if the other methionine was mono-oxidized. Moreover, the formation of a sulfonic acid derivative of γC89 was determined after $^1O_2$ exposure (Fig. 3D). As discussed in Section 4.4, oxidation of γM95 in this particular fragment was also found in non-exposed samples (Supplementary Fig. S1D).

Additionally, in the CF1 β subunit critical residues, such as βY362 (Supplementary Fig. S2A) and βH384/βY385 (Supplementary Fig. S2C), were oxidized as well. These two tyrosines, which correspond to bovine MF1 βY345 and βY368, are residues of the catalytic and non-catalytic nucleotide binding site, respectively [50]. Recently, it was shown that both β-tyrosines are the primary targets responsible for nitrative stress susceptibility, whereas γ-methionine modification was not detected [51,52].

In general, ROS treatment resulted mainly in oxidation of α, β and γ subunits, whereas degrees of δ and ε subunit oxidation were less affected (Supplementary Fig. S3).

In a second approach, CF1 oxidation was analyzed after exposure to H_2O_2. Comparable to $^1O_2$, H_2O_2-induced oxidation of C-terminal γM279 and γM282 (Supplementary Fig. S4A, B) and γC89 (Supplementary Fig. S4C) was observed. Furthermore, tri-oxidation of regulatory γC199 (Supplementary Fig. S4D) was discovered. Unfortunately, the fragment containing γM23 could not be detected in treated samples, neither in a modified nor in a non-modified state.

3.4. The effect of oxyanions on MgATP hydrolysis of hybrid F1

In this study, a hybrid F1 was assayed consisting of RrF1 $\alpha_3\beta_3$ hexamer and wild type or modified spinach CF1 γ subunits. Due to mutual oxidations (see Section 3.3), single mutants of γM279 and γM282 were not investigated. Regarding the cluster residues (Fig. 2C), methionines were substituted by leucines and cysteine by alanine, respectively, since homologous γM23L and γC89A showed minimal pertubations in *E. coli* [18]. According to numerous studies, the region of the proposed ROS targets, especially γM23 itself [18,53–55], plays a critical role in enzyme functionality. For this reason, attempts were made to characterize the hybrid F1 mutants apart from ROS response.

Firstly, the effect of oxyanions was analyzed. *In vivo* release of inhibitory MgADP is facilitated by the transmembrane proton gradient when F1 is attached to the membrane [56]. *In vitro*, the inhibitory effect of MgADP can be overcome by addition of oxyanions, such as sulfite [57,58]. Thus, enhanced MgATPase by sulfite addition was analyzed and compared to enzymes with a mutated γ subunit (Table 1). After addition of sulfite, wild type assemblies displayed a roughly fourfold increase in MgATPase activity. This was in line with previous observations of hybrid F1 under similar experimental conditions [39]. Methionine mutations significantly enhanced the stimulatory effect of sulfite. Sulfite stimulation in γC89A mutants was indistinguishable from wild type assemblies. Accordingly, the quadruple cluster mutant γM23 + 279 + 282 L/γC89A revealed no substantially additive stimulatory effect by its γC89A substitution when compared to γM23 + 279 + 282 L.

3.5. The effect of γ disulfide redox-modulation on MgATP hydrolysis by hybrid F1

In higher plant chloroplasts, ATP hydrolysis is regulated by two γ-cysteines, designated as C199 and C205 in spinach [9]. If oxidized, both cysteines form a disulfide bridge resulting in low ATP hydrolysis whereas disulfide cleavage by reduction stimulates ATP hydrolysis. It is assumed that redox-modulation of the two regulatory γ-cysteines is accompanied by dynamic structural changes within the dithiol domain, consequently affecting inter-domain movement of the γ subunit during rotational catalysis [9,26].

Since implications on proposed inter-domain movements cannot be ruled out, a second mutant characterization attempt was made to analyze as to whether substitution of cluster residues affected catalytic properties upon γ disulfide reduction (Table 2). Consistent with previous hybrid F1 studies [21], reduction of wild type γ subunit strongly enhanced ATP hydrolysis. Substitutions of methionines restricted ATPase activation upon γ disulfide reduction (see γM23L, γM279 + 282 L and γM23 + 279 + 282 L). In the γC89A this effect was less pronounced. Reduced γC199 + 205A mutants showed lower activities compared to $CuCl_2$-treated samples. A similar effect was described previously with CF1 $\alpha_3\beta_3\gamma$ assemblies lacking the regulatory cysteine region [36]. In that case, alkylation of remaining thiols in the enzyme, followed by reduction, blocked inhibition by DTT. However, hybrid F1 γC199 + 205A in our study still showed DTT-induced inhibition despite alkylation of the remaining γ-cysteines with N-ethylmaleimide prior to the reduction step (not shown).

In summary, mutual interactions within the cluster became evident. At first glance, γC89 seemed to play a minor role in sulfite stimulation (Section 3.4) and γ subunit redox-modulation. Likewise, MgATPase activity of γC89A was similar to wild type. However, γC89A was deleteriously

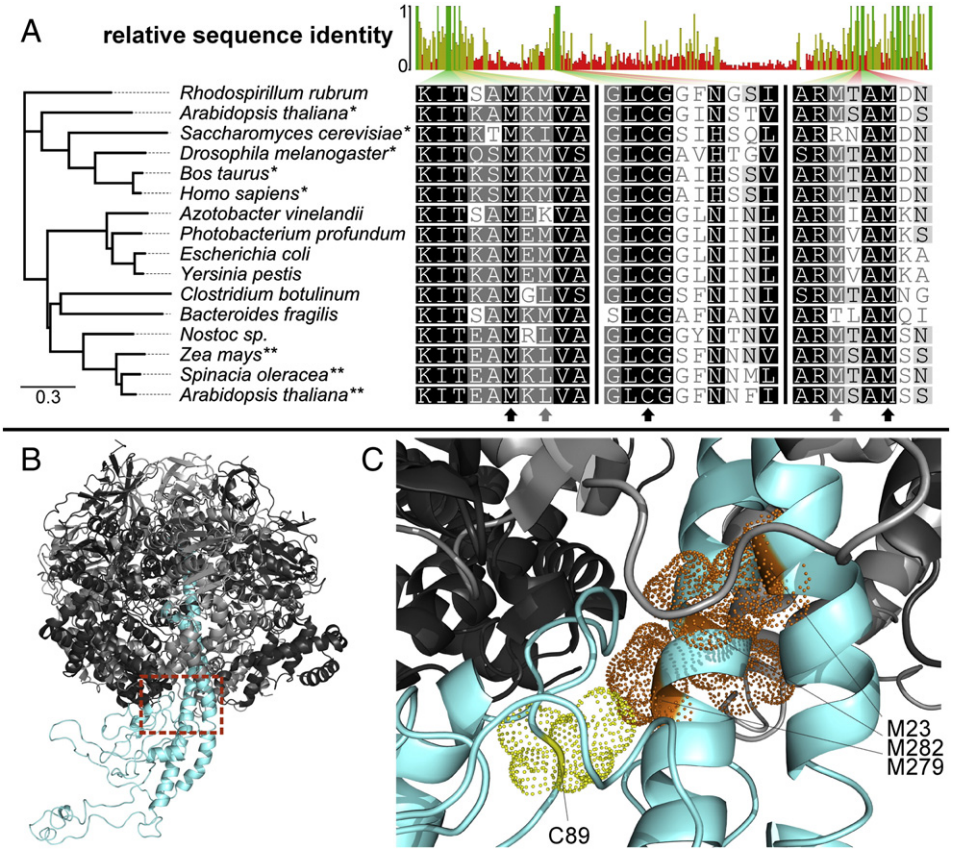

Fig. 2. (A) Amino acid sequence alignment and phylogenetic tree of 16 bacterial, mitochondrial (*) and chloroplast (**) F-ATP synthase γ subunits using ClustalW/Geneious. The scale bar represents the number of amino acid substitutions per site. The upper part shows a full sequence alignment overview with identical (green), semi-conserved (olive) and non-conserved (red) regions. Three alignment excerpts of the N-terminus, the central region and the C-terminus are shown in the lower part. Decreasing similarity of aligned residues is scaled from black to white background. The black and grey arrows below the N-terminal sequence TxxMx[MLIK]V indicate conserved (spinach γM23) and semi-conserved methionines, respectively. The black arrow below the central domain excerpt marks a conserved cysteine (spinach γC89). The grey and black arrows below the C-terminal sequence R[MRT]xAMx highlight semi-conserved (spinach γM279) and conserved (spinach γM282) methionines, respectively. (B) Alignment of crystal structures from spinach CF1 α (light grey) and β (dark grey) subunits and the γ subunit homology model (cyan) was carried out as described under Materials and methods. (C) Magnification of the dashed square from (B) shows the conserved cluster of terminal methionines in orange and the central cysteine in yellow.

dominant over methionine mutations since the cysteine substitution caused a 2-fold decrease of MgATPase when comparing the quadruple γM23 + 279 + 282 L/γC89A with the highly active γM23 + 279 + 282 L. In fact, γM23 + 279 + 282 L displayed 1.5-fold MgATPase activity than wild type. The triple mutant appeared to be highly active due to a beneficially dominant γM23L mutation, which recovered poor activity of γM279 + 282 L. Similarly, in an earlier study the interaction between these particular alpha-helical regions of *E. coli* F1 γ subunit has been described [59]. Therein, recovery of energy coupling in the deficient γM23K could be demonstrated by introducing a second γR242C mutation. EcF1 γR242 is the homolog to spinach CF1 γR278.

3.6. ATPase activity of hybrid F1 assemblies exposed to singlet oxygen

An empirical approach was undertaken by assembling hybrid F1 enzymes lacking residues that were modified by $^1O_2$ in CF1 (Fig. 3, Supplementary Fig. S2). Firstly, it turned out that substitution of oxidized β subunit residues in the nucleotide binding site did not alter $^1O_2$ response of the assemblies (Supplementary Fig. S2E), suggesting that oxidations within nucleotide binding sites played a minor role in enzyme affection. However, activity measurements of γ subunit methionine–cysteine cluster mutants (Fig. 4A) showed that these assemblies were differently affected by $^1O_2$. The most striking resistance was observed in the γM23L enzyme, whereas γC89A even tended to be slightly more susceptible to $^1O_2$ than wild type. The resistance of enzymes harboring variants of γM279 + 282 L was, if at all, only slightly higher than the wild type. Gain of γM23L resistance was preserved, if combined with wild type-like γM95L in γM23 + 95 L assemblies (Fig. 4B).

Since disulfides can be generated upon protein exposure to certain ROS [49], a γC199 + 205A construct [36] was assayed (Fig. 4B) which lacks the disulfide-forming regulatory cysteines. It turned out that this assembly was slightly more susceptible to $^1O_2$ than the wild type, indicating that activity attenuation was not a result of successive $^1O_2$-mediated disulfide formation between γC199 and γC205. In contrast to a previous proposal [12], substituting the conserved single γ-histidine with glutamine in the γH187Q did not alter the response, demonstrating that the histidine was not a functional target of $^1O_2$.

One particular feature of $^1O_2$ targets are pH-dependent reaction rate constants [60]. Especially histidines react more slowly at lower pH [45,61]. Slightly different results with even more resistant cluster mutants were obtained when exposure to $^1O_2$ was carried out at pH 6.0 (Fig. 4C) instead of pH 8.0 (as in Fig. 4A). The wild type and the γM23L mutant showed almost no pH-dependent tolerance effect. Only minor differences were observed if γC89A was analyzed at different pH, being slightly more tolerant toward oxidation at pH 6.0. The remaining multiple cluster mutants were significantly less sensitive

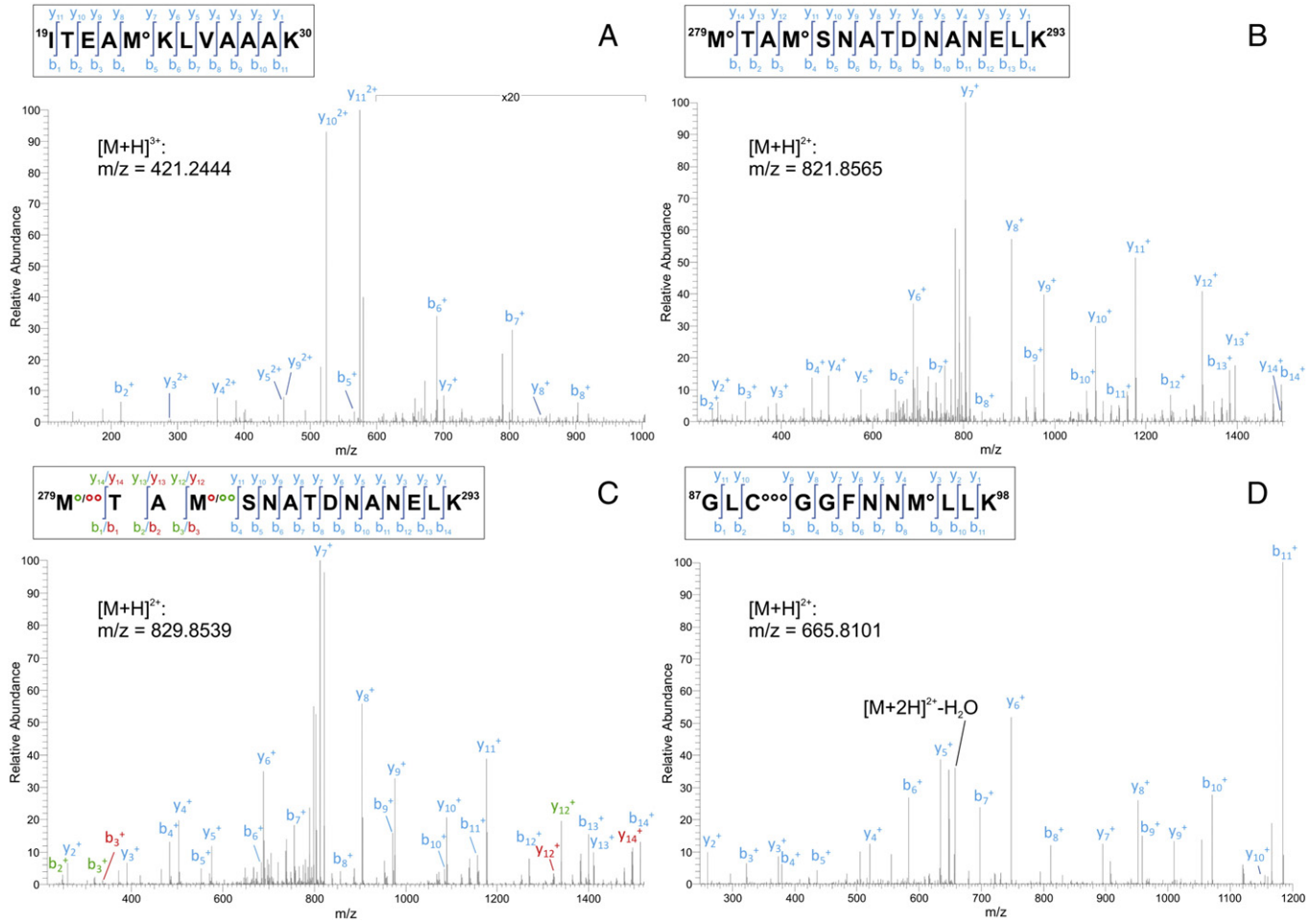

Fig. 3. Mass spectrometric analysis of singlet oxygen-induced γ subunit modifications of the conserved methionine–cysteine cluster. NanoLC–ESI/MS/MS average spectra of γ subunit peptides are shown, highlighting mono-oxidation (°), di-oxidation (°°) and tri-oxidation (°°°), respectively. The b- and y-ion series are labeled. (A) Peptide ^{19}ITEAMKLVAAAK^{30} contained mono-oxidized γM23. (B) Peptide ^{279}MTAMSNATDNANELK^{293} contained both mono-oxidized γM279 and γM282. (C) Peptide ^{279}MTAMSNATDNANELK^{293} was mono-oxidized on γM279 and di-oxidized on γM282. Alternatively, γM279 was di-oxidized and γM282 was mono-oxidized. Both cases could be distinguished with the y_{12}–y_{14} ions and with the b_1–b_3 ions. The typical ions for both possibilities were present in this MS/MS indicating both detected modifications. Green b- and y-ions: typical ions for γM279 mono-oxidized and γM282 di-oxidized; red b- and y-ions: typical ions for γM279 di-oxidized and γM282 mono-oxidized. (D) The peptide ^{87}GLCGGFNNMLLK^{98} was tri-oxidized on γC89 and mono-oxidized on γM95.

when exposed to $^1O_2$ at lower pH. Interestingly, all mutants harboring γM279 + 282 L revealed maximum increase in tolerance at pH 6. There was a slight indication of an additive effect in the triple γM23 + 279 + 282 L mutant assembly compared to the corresponding terminal mutants γM23L and γM279 + 282 L. Furthermore, substitution of γC89A had no additional effect in the quadruple γM23 + 279 + 282 L/γC89A mutant compared to γM23 + 279 + 282 L.

Table 1
The stimulatory effect of sulfite on MgATP hydrolysis of hybrid F1.

Protein preparation[a]	MgATPase activity[b]		Sulfite stimulation factor[c]
	− Sulfite	+ Sulfite	
$\alpha_3\beta_3\gamma^{\text{wild type}}$	9.5 ± 0.3	41.0 ± 0.5	4.3
$\alpha_3\beta_3\gamma^{\text{M23L}}$	4.8 ± 0.2	36.3 ± 0.7	7.6
$\alpha_3\beta_3\gamma^{\text{M279+282L}}$	2.1 ± 0.3	23.5 ± 0.3	11.2
$\alpha_3\beta_3\gamma^{\text{M23+279+282L}}$	5.9 ± 0.4	61.4 ± 0.5	10.5
$\alpha_3\beta_3\gamma^{\text{C89A}}$	8.1 ± 0.3	34.6 ± 0.4	4.3
$\alpha_3\beta_3\gamma^{\text{M23+279+282L/C89A}}$	1.9 ± 0.3	26.6 ± 0.3	14.2
$\alpha_3\beta_3\gamma^{\text{C199+205A}}$	16.7 ± 0.4	61.1 ± 0.2	3.7

[a] Hybrid F1 assemblies were purified and assayed as described under Materials and methods.
[b] Expressed as μmol Pi released min^{-1} mg $protein^{-1}$. Assay conditions as described under Materials and methods. Errors are standard errors with $n = 3$. 25 mM Na_2SO_3 was present where indicated.
[c] The stimulation factor describes the ratio of MgATPase activity in the presence of sulfite to the activity without sulfite.

Table 2
The response of γ subunit mutants to reducing/oxidizing conditions.

Protein preparation[a]	MgATPase activity[b]		Reduced/oxidized[c]
	Reduced	Oxidized	
$\alpha_3\beta_3\gamma^{\text{wild type}}$	90.0 ± 0.6	52.0 ± 1.0	1.73
$\alpha_3\beta_3\gamma^{\text{M23L}}$	57.9 ± 0.8	57.7 ± 0.8	1.00
$\alpha_3\beta_3\gamma^{\text{M279+282L}}$	27.8 ± 0.6	29.1 ± 1.1	0.96
$\alpha_3\beta_3\gamma^{\text{M23+279+282L}}$	81.3 ± 0.9	81.8 ± 0.9	0.99
$\alpha_3\beta_3\gamma^{\text{C89A}}$	77.9 ± 1.8	55.9 ± 0.9	1.39
$\alpha_3\beta_3\gamma^{\text{M23+279+282L/C89A}}$	44.2 ± 0.9	41.1 ± 0.8	1.08
$\alpha_3\beta_3\gamma^{\text{C199+205A}}$	78.6 ± 0.7	99.0 ± 0.5	0.79

[a] Hybrid F1 assemblies were purified and assayed as described under Materials and methods.
[b] Expressed as μmol Pi released min^{-1} mg $protein^{-1}$. Assay conditions as described under Materials and methods. Errors are standard errors with $n = 3$. 25 mM Na_2SO_3 was present.
[c] Reduction (10 mM DTT) and oxidation (100 μM $CuCl_2$) was carried out for 60 min and 37 °C. Ratios of reduced to oxidized MgATPase is shown.

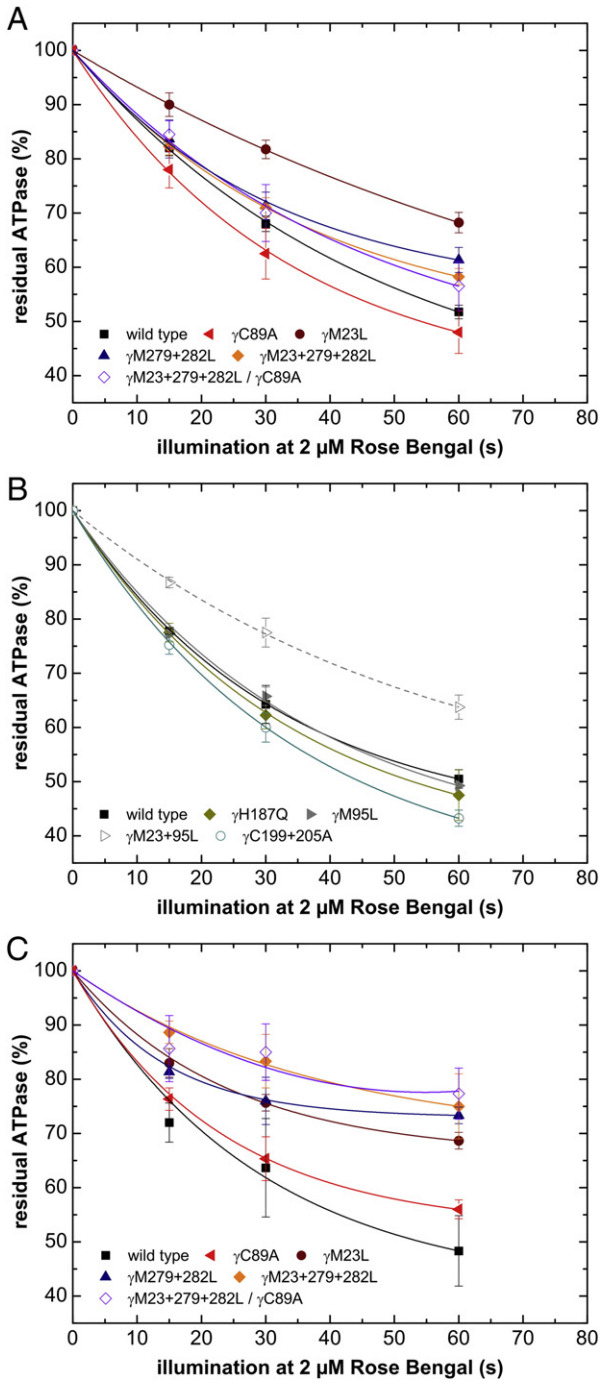

Fig. 4. Singlet oxygen lowered the MgATP hydrolysis activity of recombinant hybrid F1 assemblies. Residual activities (±standard deviation) relative to the control were plotted against exposure time. (A) Combinations of γ-methionine–cysteine cluster mutants were compared to wild type ($^1O_2$ generation at pH 8.0, $n=4$). (B) No effect was observed by substituting γM95 since affection of γM95L and γM23 + 95 L mutant was similar to wild type and γM23L from (A). The activity of γH187Q mutant declined comparably to wild type assemblies, whereas γC199 + 205A was slightly more susceptible ($^1O_2$ generation at pH 8.0, $n=4$). (C) Effect of the pH on $^1O_2$-exposed combinations of γ-methionine–cysteine cluster mutants compared to wild type (pH 6.0, $n=3$).

3.7. ATPase activity of hybrid F1 assemblies exposed to hydrogen peroxide

In a second approach we exposed cluster-substituted hybrid F1 with hydrogen peroxide. Comparable to $^1O_2$, hydrogen peroxide led to a substantial decrease in activity of hybrid F1 wild type. The data indicated that a significant decrease in activity resulted from oxidation of the cluster residues (Fig. 5A). Similar tolerances could be observed for γC89A, γM279 + 282 L and γM23 + 279 + 282 L, respectively. Absence of γM23 led to a small decrease in inhibition only. Similarly, neither enhanced tolerance by γM23L was observed in the triple mutant γM23 + 279 + 282 L, when compared to γM279 + 282 L, nor in the almost H_2O_2-tolerant γM279 + 282 L/γC89A. However, the most striking effect was observed in the quadruple cluster mutant γM23 + 279 + 282 L/γC89A that rendered the enzyme virtually insensitive to H_2O_2. Surprisingly, exposing wild type to lower concentrations of 1 mM H_2O_2 (Fig. 5B) yielded a slightly activated enzyme which showed successive ATPase attenuation with increasing H_2O_2 concentrations. The quadruple cluster mutant γM23 + 279 + 282 L/γC89A showed a higher extent of activation with little inhibition occurring at higher H_2O_2 concentrations. The absence of the non-target histidine in γH187Q had no effect on susceptibility (Fig. 5C). Albeit a sulfonic acid derivative of a regulatory cysteine could be detected (Supplementary Fig. S4D), no implications on H_2O_2 tolerance were observed for γC199 + 205A (Fig. 5C).

3.8. Sulfite stimulation upon exposure to reactive oxygen species

As shown in this study, even minimally perturbing mutations of the γ subunit methionine–cysteine cluster dramatically changed catalytic properties and ROS sensitivity of the enzyme. It remained elusive by which means ROS provoked activity decline. One possibility among others could be that reactive oxygen affects MgADP binding and release. However, it was evident that exposure to $^1O_2$ had only marginal influence on MgATPase stimulation by sulfite in the wild type (Table 3).

Since the data in Fig. 5A suggested that H_2O_2-induced enzyme affection was caused by oxidation of the γ subunit methionine–cysteine cluster, γM23 + 279 + 282 L/γC89A served as control in the H_2O_2-dependent sulfite stimulation assay shown in Table 4. Again, the data obtained did not reveal H_2O_2-induced changes of the sulfite effect on MgATPase. Nevertheless, both the wild type enzyme and the quadruple mutant showed a small increase of sulfite-induced H_2O_2 resistance.

4. Discussion

4.1. Impact of singlet oxygen on enzyme activity in situ and in vitro

Under daylight conditions, when ROS are continuously generated as a natural byproduct of photosynthesis, CF1CFO primarily acts as an ATP synthase. A decreased photophosphorylation capacity of thylakoids upon oxidative stress could potentially alter ADP/ATP ratios *in vivo*, which then might function as a signal. Promotion of excessive membrane uncoupling under the assayed conditions can be ruled out [12]. The *in vitro* data suggested that observed $^1O_2$-induced attenuation *in situ* involved impairment of CF1 activity. Disproving earlier suggestions [12], the results did not support cross-link events between residues of the γ and ε subunits upon $^1O_2$ exposure. The mutant studies presented in this work were performed with recombinant hybrid F1 assemblies. These enzymes acquired γ subunit features unique to higher plants. The assembly system was considered to be a suitable tool for ROS-dependent γ subunit modifications since it exhibited similar MgATPase activation upon γ disulfide reduction as native CF1 $\alpha_3\beta_3\gamma$ assemblies [36]. If activity attenuation in CF1/CF1-δε (Fig. 1B) would have been primarily caused by ROS-induced modifications of the γ subunit, these alterations should have had a similar impact on activity in the hybrid F1 assembly.

4.2. Mass spectrometry analysis of CF1 oxidation

The sulfur-containing amino acid cluster was highly susceptible to $^1O_2$ and most residues of the cluster were also oxidized by H_2O_2, although

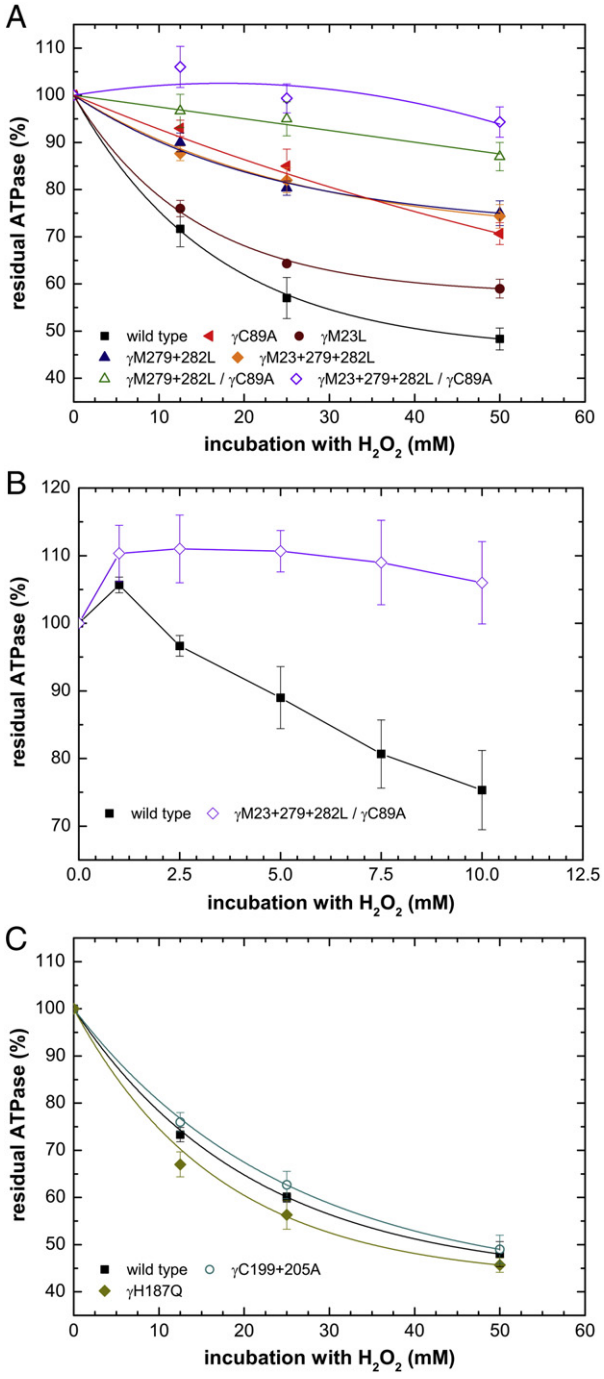

Fig. 5. Hydrogen peroxide lowered the MgATP hydrolysis activity of recombinant hybrid F1 assemblies. Residual activities (±standard deviation, $n=3$) relative to the control were plotted against exposure to increasing concentrations of H_2O_2. (A) Combinations of γ-methionine–cysteine cluster mutants were compared to wild type. (B) Comparison of wild type with γM23 + 279 + 282 L/γC89A at lower concentrations of H_2O_2. One millimolar H_2O_2 caused a slight initial ATPase activation of 10% and 6% observed in γM23 + 279 + 282 L/γC89A and the wild type assembly, respectively. With increasing concentrations the assemblies showed activities as outlined in (A). (C) The activity of γH187Q and γC199 + 205A assemblies declined comparably to γ wild type enzyme.

peptides containing γM23 could not be detected in H_2O_2-treated samples. Regarding γM279 and γM282, a mutual oxidation pattern was observed, similar to results obtained previously using methionine–methionine dipeptides [62]. Therefore, single mutants of these particular residues were not analyzed. The two regulatory γC199 and γC205 were

Table 3
The stimulatory effect of sulfite on MgATP hydrolysis of $^1O_2$-exposed hybrid F1 wild type.

$^1O_2$ release by RB[a]	MgATPase activity[b]		Residual activity[c]		Sulfite stimulation factor[d]
	− Sulfite	+ Sulfite	− Sulfite	+ Sulfite	
0 s	8.7 ± 0.3	36.0 ± 0.6	100%	100%	4.1
15 s	6.8 ± 0.3	28.9 ± 0.8	78%	80%	4.3
60 s	4.7 ± 0.1	17.1 ± 0.4	54%	48%	3.6

[a] Singlet oxygen was released at pH 8.0 during illumination in the presence of 2 μM RB.
[b] Expressed as μmol Pi released min^{-1} mg $protein^{-1}$. Assay conditions as described under Materials and methods. Errors are standard errors with $n=3$. 25 mM Na_2SO_3 was present where indicated.
[c] The value was obtained by setting activity after $^1O_2$ treatment relative to activity of the nontreated control.
[d] The stimulation factor describes the ratio of MgATPase activity in the presence of sulfite to the activity without sulfite.

not affected by $^1O_2$ (not shown), whereas H_2O_2 treatment resulted in severe oxidation, in particular γC199. The initially proposed main target for ROS impact γH187 [12] was not oxidized.

4.3. The effects of oxyanions and γ disulfide redox-modulation on MgATP hydrolysis of hybrid F1 and its mutants

The results we obtained with the alpha-helical methionine mutants were in good agreement with earlier studies describing MgATPase activation by detergent-stimulated MgADP release in TF1 $\alpha_3\beta_3\gamma$ from the thermophilic *Bacillus* PS3 [54]. Therein, homologous residues to spinach CF1 γM23 and γM282 were substituted for cysteine or lysine. Similarly, a study of *Rhodobacter capsulatus* F1 [55] proposes a stabilization of the ADP-inhibited state of the enzyme by γM23K. All of these studies point into the direction that integrity of this alpha-helical γ-region is crucial for ADP release during rotation [21,54,55,63], probably because it is part of a β-γ contact point [19–21]. Alternatively, other electrostatic [55,64,65] or hydrophobic [54] parameters might also play a role.

Table 4
The stimulatory effect of sulfite on MgATP hydrolysis of H_2O_2-exposed hybrid F1.

Protein preparation[a]	Na_2SO_3	MgATPase activity[c]				Resistance factor[d]
		−		+		
	H_2O_2[b]	−	+	−	+	
$\gamma^{wild\ type}$		7.9 (±0.3)	2.7 (±0.2)	33.1 (±0.2)	15.0 (±0.2)	1.3
	Residual activity[e]		34%		45%	
	Sulfite stimulation factor[f]		4.2		5.6	
$\gamma^{M23+279+282L/C89A}$		2.7 (±0.3)	2.1 (±0.1)	26.8 (±0.4)	23.4 (±0.2)	1.1
	Residual activity[e]		78%		87%	
	Sulfite stimulation factor[f]		9.8		11.0	

[a] Hybrid F1 assemblies were purified and assayed as described under Materials and methods.
[b] H_2O_2 treatment (50 mM) is described under methods.
[c] Expressed as μmol Pi released min^{-1} mg $protein^{-1}$. Assay conditions as described under Materials and methods. Errors are standard errors with $n=3$. 25 mM Na_2SO_3 was present where indicated.
[d] The resistance factor describes the ratio of residual activity upon H_2O_2 in the presence of sulfite to residual activity without sulfite.
[e] The value was obtained by setting activity after H_2O_2 treatment relative to activity of the non-treated control.
[f] The stimulation factor describes the ratio of MgATPase activity in the presence of sulfite to the activity without sulfite.

By substituting leucine for methionine and alanine for cysteine, the hydrophobic character of the cluster was preserved to a certain extent. According to our results, hydrophobicity of the substituted γ-residues appeared to have a minor impact on the oxyanion effect. However, substitution of alpha-helical methionines had the most dramatic consequence on sulfite stimulation and γ subunit redox-modulation. Regarding the latter, these residues must somehow relay the information produced by disulfide reduction, since the methionines are not part of the actual regulatory domain. Nevertheless, the observations on γ disulfide redox-modulation did not take account of the ε subunit which is also considered to regulate activity [9].

Summarizing the additional experiments apart from ROS response, it turned out that the introduced amino acid substitutions had an impact on the activity of the enzyme. As shown for yeast MF1, αF405S induced positional changes of the β and the γ subunit, in particular the γC84-containing conserved central loop [66]. Therein, the authors suggest that lower β–γ catch interactions were affected. Therefore, analogous remote structural impacts in hybrid F1 γ subunit mutants cannot be ruled out. Our results also suggested that the cluster appeared to be a set of highly dynamic interacting residues. The effect of certain substitutions was obviously dominant over others. All of these conclusions have to be drawn with caution, since the observed activities only allow limited predictions of membrane-attached enzyme characteristics.

4.4. ATPase activity of hybrid F1 assemblies exposed to singlet oxygen

Establishing a connection between the potential role of F-ATP synthase in maintaining ROS homeostasis [15,16] and its concurrent susceptibility [10–12] is challenging. Unlike previous experiments analyzing nitrative stress [51,52], susceptibility of F-ATPase caused by ROS could not be linked to any specific amino acid targets. However, recent studies of fungal mitochondrial F1 identified a selected tryptophan on the α subunit as a functional ROS target [67]. The results presented here revealed that (1) all of the mutants tested still showed significant activity attenuation upon $^1O_2$ exposure, and (2) that this effect is mainly dependent on the oxidation of the methionine–cysteine cluster. (3) This cluster appeared as a group of mutually dependent residues. Therefore, we suggest that the cluster should rather be regarded as a whole target system. Accordingly, three possible conclusions could be drawn to interpret the results in Fig. 4. (a) Changing the cluster by partial mutation might cause altered catalytic impact upon oxidation. As a result, increased sensitivity in γC89A could be observed. Likewise, formerly tolerant γM23L was not persistent in γM23 + 279 + 282 L due to enhanced deleterious impact of the latter oxidized disrupted target cluster. (b) Enduring susceptibility of γM23 + 279 + 282 L/γC89A strongly demanded for existence of functional targets remote of the suggested cluster. At least oxidized nucleotide binding site residues within the β subunit were not involved in loss of enzyme activity. The challenge of identifying yet unknown functional targets is aggravated since oxidation of a residue can also occur spontaneously and without affecting the enzyme functionality [68,69], as shown for γM95. (c) In line with previous reports, the cluster region appeared to be critical for general enzyme functionality. It is likely that the introduced mutations might have the potential to affect remote functional structures (Section 4.3). Accordingly, it cannot be ruled out that concealed potential $^1O_2$ target residues were experimentally changed to functional $^1O_2$ targets. Theoretically, this would challenge conclusion (a) by implying that cluster residues themselves are supposedly "concealed" in the wild type and only become "functional" in disrupted cluster mutants. Nevertheless, every single cluster residue was specifically oxidized upon $^1O_2$ treatment (Section 3.3) and modified experimental conditions at lower pH undermine theoretical restrictions of concealed targets within the cluster itself. Taking this into consideration, overlapping of both possibilities still cannot be excluded. Candidates which might serve as new functional ROS targets could be highly reactive histidines. Several observations supported this assumption. Analyzing this amino acid, we took advantage of the fact that histidine reacts much slower at non-physiological lower pH [45,61,70]. Accordingly, lowering histidine reactivity at pH 6 in hybrid F1 wild type did not alter susceptibility. Thus, and as suggested, new functional targets appeared only in the mutants. However, in the wild type these histidines might be subject to oxidation without substantial catalytic impact. As measured by gain of $^1O_2$ tolerance at pH 6, the mutants were differently efficient in evoking histidine targets. Hence, steadily tolerant γM23L was less and mutants harboring variants of γM279 + 282 L appeared to be most efficient in functionalizing targets. Nevertheless, carefully evaluating the experimental outcome, one has to take into account that artifact-prone results might be obtained as a consequence of provoked modest structural changes in the mutants together with the intense reactivity of $^1O_2$. Regarding the latter, assemblies were exposed to less reactive oxidants as well.

4.5. ATPase activity of hybrid F1 assemblies exposed to hydrogen peroxide

Recently [71], $^1O_2$ was considered the most potent ROS involved in photo-oxidative damage in plants, whereas its reactivity with proteins is not fully understood yet [45,72,73]. The interaction of H_2O_2 with proteins is less versatile since it reacts with cysteines and methionines only, thus serving as a poor oxidant [74]. The initially proposed existence of a ROS-sensitive γ subunit amino acid cluster was clearly validated in the H_2O_2 approach. However, the molecular basis of the slight activation upon H_2O_2 exposure remained elusive. It seemed to be that slight initial activation was caused by oxidation processes apart from the ROS target residue cluster. Compared to γM23 + 279 + 282 L/γC89A, in wild type assemblies the consequence of cluster oxidation was a less pronounced slight activation, followed by activity decline at higher concentrations H_2O_2.

Regardless of yet unknown targets, it should be noted that the ultimate fate of ROS exposure was a loss of enzyme activity. On the other hand, the aftereffects of amino acid oxidations within a disrupted cluster seemed to be different, depending on the ROS applied. Especially absence of γM23 and γC89 during oxidative enzyme modification resulted in inverted responses upon $^1O_2$ and H_2O_2 stress (Figs. 4C, 5A). In this context it should be noted that sulfite-stimulated MgATPase of γM23L and γC89A were most similar to wild type (Table 1). According to the conclusions proposed above (Section 4.4), ROS-specific reactivity of formerly concealed targets could cause inverted responses. Additionally, ROS-specific impact of a γM23- and γC89-disrupted cluster on catalytic activity should be considered.

4.6. Sulfite stimulation upon exposure to reactive oxygen species

The critical location of the cluster (Fig. 2C), its involvement in dynamic wide-ranging interactions within the enzyme (Tables 1 and 2) and its susceptibility to ROS (Fig. 3, Supplementary Fig. S4) were clearly evident. Nevertheless, the detailed molecular mechanism of how the detrimental cluster target oxidation affects structure and function remained elusive. Although methionine sulfoxide is more hydrophilic than methionine [49] and some authors consider hydrophobicity of the cluster region to be involved in MgADP release [54], no enhanced sulfite stimulation upon ROS exposure could be observed. Previously, it was described that methionine sulfoxide formation in alpha-helical regions of proteins can have helix-breaking effects [75]. Assuming that this might be the case at least for γM279 and γM282, C-terminal catch interactions with an anionic loop of the β subunit [19] could be disordered. In line with this assumption, previous hybrid F1 studies of C-terminal γ subunit mutants showed loss of MgATPase [39].

In summary, we could present evidence that oxidation of a conserved group of interacting subunit residues was responsible for H_2O_2-induced activity attenuation. It is very likely that additional residues participated in $^1O_2$-dependent loss of activity. Therefore, future studies might be helpful to identify additional functional targets and

further unravel the molecular mechanism of ROS-induced catalytic activity decay. Since this markedly conserved group of highly ROS-sensitive amino acids is located at a critical position and of functional importance, it is tempting to speculate if these key residues might serve as a sensor for increasing ROS concentrations. Thus, affection of ADP/ATP ratio and/or the thylakoid ΔpH might have further implications on the regulation of the photosynthetic machinery in general.

Author contributions

F.B., M.L.R. and C.F. designed research, F.B. and Y.S. performed research, F.B., Y.S., A.R., M.L.R. and C.F. analyzed data, F.B., M.L.R. and C.F. wrote the paper.

Acknowledgements

This work was funded by an EMBO fellowship (ASTF 292-2010) granted to F.B. and the Justus-Liebig-University, Giessen. Instrumental support by Zoltan Takats (ERC Starting Grant "DESI_JeDI Imaging") and Bernhard Spengler (DFG Sp314/12-1) is gratefully acknowledged.

Appendix A. Supplementary data

Supplementary data to this article can be found online at http://dx.doi.org/10.1016/j.bbabio.2012.06.007.

References

[1] K. Apel, H. Hirt, Reactive oxygen species: metabolism, oxidative stress, and signal transduction, Annu. Rev. Plant Biol. 55 (2004) 373–399.
[2] Y. Nishiyama, S.I. Allakhverdiev, N. Murata, A new paradigm for the action of reactive oxygen species in the photoinhibition of photosystem II, Biochim. Biophys. Acta 1757 (2006) 742–749.
[3] C.H. Foyer, G. Noctor, Leaves in the dark see the light, Science 284 (1999) 599–601.
[4] R. Mittler, Oxidative stress, antioxidants and stress tolerance, Trends Plant Sci. 7 (2002) 405–410.
[5] G.P. Bienert, J.K. Schjoerring, T.P. Jahn, Membrane transport of hydrogen peroxide, Biochim. Biophys. Acta 1758 (2006) 994–1003.
[6] B.B. Fischer, A. Krieger-Liszkay, E. Hideg, I. Snyrychova, M. Wiesendanger, R.I. Eggen, Role of singlet oxygen in chloroplast to nucleus retrograde signaling in *Chlamydomonas reinhardtii*, FEBS Lett. 581 (2007) 5555–5560.
[7] S. Neill, R. Desikan, J. Hancock, Hydrogen peroxide signalling, Curr. Opin. Plant Biol. 5 (2002) 388–395.
[8] C. Kim, R. Meskauskiene, K. Apel, C. Laloi, No single way to understand singlet oxygen signalling in plants, EMBO Rep. 9 (2008) 435–439.
[9] M.L. Richter, γ–ε interactions regulate the chloroplast ATP synthase, Photosynth. Res. 79 (2004) 319–329.
[10] Y. Zhang, O. Marcillat, C. Giulivi, L. Ernster, K.J.A. Davies, The oxidative inactivation of mitochondrial electron-transport chain components and ATPase, J. Biol. Chem. 265 (1990) 16330–16336.
[11] G. Lippe, M. Comelli, D. Mazzilis, F.D. Sala, I. Mavelli, The inactivation of mitochondrial F1 ATPase by H_2O_2 is mediated by iron ions not tightly bound in the protein, Biochem. Biophys. Res. Commun. 181 (1991) 764–770.
[12] F. Buchert, C. Forreiter, Singlet oxygen inhibits ATPase and proton translocation activity of the thylakoid ATP synthase CF1CFo, FEBS Lett. 584 (2010) 147–152.
[13] J. Glaeser, A.M. Nuss, B.A. Berghoff, G. Klug, Singlet oxygen stress in microorganisms, Adv. Microb. Physiol. 58 (2011) 141–173.
[14] V. Adam-Vizi, C. Chinopoulos, Bioenergetics and the formation of mitochondrial reactive oxygen species, Trends Pharmacol. Sci. 27 (2006) 639–645.
[15] J. Houstek, A. Pickova, A. Vojtiskova, T. Mracek, P. Pecina, P. Jesina, Mitochondrial diseases and genetic defects of ATP synthase, Biochim. Biophys. Acta 1757 (2006) 1400–1405.
[16] A. Kanazawa, D.M. Kramer, *In vivo* modulation of nonphotochemical exciton quenching (NPQ) by regulation of the chloroplast ATP synthase, Proc. Natl. Acad. Sci. U. S. A. 99 (2002) 12789–12794.
[17] H. Mahler, P. Wuennenberg, M. Linder, D. Przybyla, C. Zoerb, F. Landgraf, C. Forreiter, Singlet oxygen affects the activity of the thylakoid ATP synthase and has a strong impact on its γ subunit, Planta 225 (2007) 1073–1083.
[18] K. Shin, R.K. Nakamoto, M. Maeda, M. Futai, FoF1-ATPase γ subunit mutations perturb the coupling between catalysis and transport, J. Biol. Chem. 267 (1992) 20835–20839.
[19] J.P. Abrahams, A.G. Leslie, R. Lutter, J.E. Walker, Structure at 2.8 A resolution of F1-ATPase from bovine heart mitochondria, Nature 370 (1994) 621–628.
[20] J.Z. Pu, M. Karplus, How subunit coupling produces the γ subunit rotary motion in F-1-ATPase, Proc. Natl. Acad. Sci. U. S. A. 105 (2008) 1192–1197.
[21] H.S. Samra, F. He, N.R. Degner, M.L. Richter, The role of specific β–γ subunit interactions in oxyanion stimulation of the MgATP hydrolysis of a hybrid photosynthetic F-1-ATPase, J. Bioenerg. Biomembr. 40 (2008) 69–76.
[22] M.A. Larkin, G. Blackshields, N.P. Brown, R. Chenna, P.A. McGettigan, H. McWilliam, F. Valentin, I.M. Wallace, A. Wilm, R. Lopez, J.D. Thompson, T.J. Gibson, D.G. Higgins, Clustal W and clustal X version 2.0, Bioinformatics 23 (2007) 2947–2948.
[23] A.J. Drummond, B. Ashton, S. Buxton, M. Cheung, A. Cooper, C. Duran, M. Field, J. Heled, M. Kearse, S. Markowitz, R. Moir, S. Stones-Havas, S. Sturrock, T. Thierer, A. Wilson, Geneious v5.4. Available from http://www.geneious.com/2011.
[24] W.L. DeLano, J.W. Lam, PyMOL: a communications tool for computational models, Abstr. Pap. Am. Chem. Soc. 230 (2005) U1371–U1372.
[25] I.N. Shindyalov, P.E. Bourne, Protein structure alignment by incremental combinatorial extension (CE) of the optimal path, Protein Eng. 11 (1998) 739–747.
[26] M.L. Richter, H.S. Samra, F. He, A.J. Giessel, K.K. Kuczera, Coupling proton movement to ATP synthesis in the chloroplast ATP synthase, J. Bioenerg. Biomembr. 37 (2005) 467–473.
[27] G. Groth, E. Pohl, The structure of the chloroplast F1-ATPase at 3.2 angstrom resolution, J. Biol. Chem. 276 (2001) 1345–1352.
[28] G. Cingolani, T.M. Duncan, Structure of the ATP synthase catalytic complex F1 from *Escherichia coli* in an autoinhibited conformation, Nat. Struct. Mol. Biol. 18 (2011) 701–707.
[29] R.E. McCarty, The decay of the ATPase activity of light plus thiol-activated thylakoid membranes in the dark, J. Bioenerg. Biomembr. 38 (2006) 67–74.
[30] A.B. Shapiro, R.E. McCarty, Substrate binding-induced alteration of nucleotide binding site properties of chloroplast coupling factor-1, J. Biol. Chem. 265 (1990) 4340–4347.
[31] M.L. Richter, Z. Gromet-Elhanan, R.E. McCarty, Reconstitution of the H^+-ATPase complex of *Rhodospirillum rubrum* by the β subunit of the chloroplast coupling factor-1, J. Biol. Chem. 261 (1986) 12109–12113.
[32] M.M. Bradford, Rapid and sensitive method for quantitation of microgram quantities of protein utilizing principle of protein-dye binding, Anal. Biochem. 72 (1976) 248–254.
[33] D.I. Arnon, Copper enzymes in isolated chloroplasts. Polyphenoloxidase in *Beta vulgaris*, Plant Physiol. 24 (1949) 1–15.
[34] M. Sokolov, L. Lu, W. Tucker, F. Gao, P.A. Gegenheimer, M.L. Richter, The 20 C-terminal amino acid residues of the chloroplast ATP synthase γ subunit are not essential for activity, J. Biol. Chem. 274 (1999) 13824–13829.
[35] L. Nathanson, Z. Gromet-Elhanan, Mutagenesis of β-Glu-195 of the *Rhodospirillum rubrum* F1-ATPase and its role in divalent cation-dependent catalysis, J. Biol. Chem. 273 (1998) 10933–10938.
[36] H.S. Samra, F. Gao, F. He, E. Hoang, Z.G. Chen, P.A. Gegenheimer, C.L. Berrie, M.L. Richter, Structural analysis of the regulatory dithiol-containing domain of the chloroplast ATP synthase γ subunit, J. Biol. Chem. 281 (2006) 31041–31049.
[37] W.C. Tucker, A. Schwarz, T. Levine, Z.Y. Du, Z. Gromet-Elhanan, M.L. Richter, G. Haran, Observation of calcium-dependent unidirectional rotational motion in recombinant photosynthetic F-1-ATPase molecules, J. Biol. Chem. 279 (2004) 47415–47418.
[38] F.W. Studier, B.A. Moffatt, Use of bacteriophage T7 RNA polymerase to direct selective high-level expression of cloned genes, J. Mol. Biol. 189 (1986) 113–130.
[39] F. He, H.S. Samra, W.C. Tucker, D.R. Mayans, E. Hoang, Z. Gromet-Elhanan, C.L. Berrie, M.L. Richter, Mutations within the C-terminus of the gamma subunit of the photosynthetic F-1-ATPase activate MgATP hydrolysis and attenuate the stimulatory oxyanion effect, Biochemistry 46 (2007) 2411–2418.
[40] H.S. Penefsky, Reversible binding of Pi by beef-heart mitochondrial adenosine-triphosphatase, J. Biol. Chem. 252 (1977) 2891–2899.
[41] T.Y. Lin, C.H. Wu, Activation of hydrogen peroxide in copper(II)/amino acid/H_2O_2 systems: effects of pH and copper speciation, J. Catal. 232 (2005) 117–126.
[42] H.H. Taussky, E. Shorr, A microcolorimetric method for the determination of inorganic phosphorus, J. Biol. Chem. 202 (1953) 675–685.
[43] R.E. McCarty, ATP synthase of chloroplast thylakoid membranes: a more in depth characterization of its ATPase activity, J. Bioenerg. Biomembr. 37 (2005) 289–297.
[44] M.L. Richter, W.J. Patrie, R.E. McCarty, Preparation of the ε subunit and ε subunit-deficient chloroplast coupling factor-1 in reconstitutively active forms, J. Biol. Chem. 259 (1984) 7371–7373.
[45] M.J. Davies, Singlet oxygen-mediated damage to proteins and its consequences, Biochem. Biophys. Res. Commun. 305 (2003) 761–770.
[46] R.K. Nakamoto, K. Shin, A. Iwamoto, H. Omote, M. Maeda, M. Futai, *Escherichia coli* FoF1-ATPase—residues involved in catalysis and coupling, Ann. N. Y. Acad. Sci. 671 (1992) 335–344.
[47] D. Stock, A.G.W. Leslie, J.E. Walker, Molecular architecture of the rotary motor in ATP synthase, Science 286 (1999) 1700–1705.
[48] D.M. Rees, A.G.W. Leslie, J.E. Walker, The structure of the membrane extrinsic region of bovine ATP synthase, Proc. Natl. Acad. Sci. U. S. A. 106 (2009) 21597–21601.
[49] M.J. Davies, The oxidative environment and protein damage, Biochim. Biophys. Acta 1703 (2005) 93–109.
[50] R.L. Cross, D. Cunningham, C.G. Miller, Z.X. Xue, J.M. Zhou, P.D. Boyer, Adenine-nucleotide binding-sites on beef-heart F1 ATPase—photoaffinity-labeling of β subunit Tyr-368 at a noncatalytic site and β Tyr-345 at a catalytic site, Proc. Natl. Acad. Sci. U. S. A. 84 (1987) 5715–5719.
[51] Y. Fujisawa, K. Kato, C. Giulivi, Nitration of tyrosine residues 368 and 345 in the β subunit elicits FoF1-ATPase activity loss, Biochem. J. 423 (2009) 219–231.
[52] V. Haynes, N.J. Traaseth, S. Elfering, Y. Fujisawa, C. Giulivi, Nitration of specific tyrosines in FoF1 ATP synthase and activity loss in aging, Am. J. Physiol. Endocrinol. Metab. 298 (2010) E978–E987.
[53] H. Omote, N. Sambonmatsu, K. Saito, Y. Sambongi, A. Iwamoto-Kihara, T. Yanagida, Y. Wada, M. Futai, The γ subunit rotation and torque generation in F1-ATPase from

wild-type or uncoupled mutant *Escherichia coli*, Proc. Natl. Acad. Sci. U. S. A. 96 (1999) 7780–7784.
[54] S. Bandyopadhyay, W.S. Allison, γM23K, γM232K, and γL77K single substitutions in the TF1-ATPase lower ATPase activity by disrupting a cluster of hydrophobic side chains, Biochemistry 43 (2004) 9495–9501.
[55] B.A. Feniouk, A. Rebeechi, D. Giovannini, S. Anefors, A.Y. Mulkidjanian, W. Junge, P. Tunina, A. Melandri, Met23Lys mutation in subunit γ of FoF1-ATP synthase from *Rhodobacter capsulatus* impairs the activation of ATP hydrolysis by proton motive force, Biochim. Biophys. Acta 1767 (2007) 1319–1330.
[56] Z.Y. Du, P.D. Boyer, On the mechanism of sulfite activation of chloroplast thylakoid ATPase and the relation of ADP tightly bound at a catalytic site to the binding change mechanism, Biochemistry 29 (1990) 402–407.
[57] A.N. Malyan, Chloroplasts ATPase CF1—allosteric regulation by ADP and Mg^{2+} ions, Photosynthetica 15 (1981) 474–483.
[58] M.B. Murataliev, P.D. Boyer, Interaction of mitochondrial F1-ATPase with trinitrophenyl derivatives of ATP and ADP—participation of 3rd catalytic site and role of Mg^{2+} in enzyme inactivation, J. Biol. Chem. 269 (1994) 15431–15439.
[59] R.K. Nakamoto, M. Maeda, M. Futai, The γ subunit of the *Escherichia coli* ATP synthase—mutations in the carboxyl-terminal region restore energy coupling to the amino-terminal mutant γMet-23-Lys, J. Biol. Chem. 268 (1993) 867–872.
[60] F. Wilkinson, W.P. Helman, A.B. Ross, Rate constants for the decay and reactions of the lowest electronically excited singlet-state of molecular oxygen in solution—an expanded and revised compilation, J. Phys. Chem. Ref. Data 24 (1995) 663–1021.
[61] R.H. Bisby, C.G. Morgan, I. Hamblett, A.A. Gorman, Quenching of singlet oxygen by Trolox C, ascorbate, and amino acids: effects of pH and temperature, J. Phys. Chem. A 103 (1999) 7454–7459.
[62] B.L. Miller, K. Kuczera, C. Schoneich, One-electron photooxidation of N-methionyl peptides. Mechanism of sulfoxide and azasulfonium diastereomer formation through reaction of sulfide radical cation complexes with oxygen or superoxide, J. Am. Chem. Soc. 120 (1998) 3345–3356.
[63] S.X. Sun, H.Y. Wang, G. Oster, Asymmetry in the F-1-ATPase and its implications for the rotational cycle, Biophys. J. 86 (2004) 1373–1384.
[64] M.K. Al-Shawi, C.J. Ketchum, R.K. Nakamoto, Energy coupling, turnover, and stability of the FoF1 ATP synthase are dependent on the energy of interaction between γ and β subunits, J. Biol. Chem. 272 (1997) 2300–2306.
[65] C.J. Ketchum, M.K. Al-Shawi, R.K. Nakamoto, Intergenic suppression of the γM23K uncoupling mutation in FoF1 ATP synthase by βGlu-381 substitutions: the role of the β380DELSEED386 segment in energy coupling, Biochem. J. 330 (1998) 707–712.
[66] D. Arsenieva, J. Symersky, Y. Wang, V. Pagadala, D.M. Mueller, Crystal structures of mutant forms of the yeast F1 ATPase reveal two modes of uncoupling, J. Biol. Chem. 285 (2010) 36561–36569.
[67] S. Rexroth, A. Poetsch, M. Rogner, A. Hamann, A. Werner, H.D. Osiewacz, E.R. Schafer, H. Seelert, N.A. Dencher, Reactive oxygen species target specific tryptophan site in the mitochondrial ATP synthase, Biochim. Biophys. Acta 1817 (2012) 381–387.
[68] M. Walsh, F.C. Stevens, K. Oikawa, C.M. Kay, Circular dichroism studies on Ca^{2+}-dependent protein modulator oxidized with N-chlorosuccinimide, Biochemistry 17 (1978) 3928–3930.
[69] R.L. Levine, B.S. Berlett, J. Moskovitz, L. Mosoni, E.R. Stadtman, Methionine residues may protect proteins from critical oxidative damage, Mech. Ageing Dev. 107 (1999) 323–332.
[70] H.W. Heldt, K. Werdan, M. Milovanc, G. Geller, Alkalization of chloroplast stroma caused by light-dependent proton flux into thylakoid space, Biochim. Biophys. Acta 314 (1973) 224–241.
[71] C. Triantaphylides, M. Krischke, F.A. Hoeberichts, B. Ksas, G. Gresser, M. Havaux, F. Van Breusegem, M.J. Mueller, Singlet oxygen is the major reactive oxygen species involved in photooxidative damage to plants, Plant Physiol. 148 (2008) 960–968.
[72] P. Wardman, C. Vonsonntag, Kinetic factors that vontrol the fate of thiyl radicals in cells, Methods Enzymol. 251 (1995) 31–45.
[73] A. Wright, W.A. Bubb, C.L. Hawkins, M.J. Davies, Singlet oxygen-mediated protein oxidation: evidence for the formation of reactive side chain peroxides on Tyrosine residues, Photochem. Photobiol. 76 (2002) 35–46.
[74] J.A. Imlay, Pathways of oxidative damage, Annu. Rev. Microbiol. 57 (2003) 395–418.
[75] D.J. Bigelow, T.C. Squier, Redox modulation of cellular signaling and metabolism through reversible oxidation of methionine sensors in calcium regulatory proteins, Biochim. Biophys. Acta 1703 (2005) 121–134.